

Dielectric Characteristics in Smectic Phase

Jun Ho Song¹, Suck Coi¹, Yong Bae Kim², Satyendra Kumar³, Jun Hyung Souk⁴,
and Sung Tae Shin¹

¹Department of Physics and Applied Physics, Korea University, Seoul 136-701, Korea

²Department of Chemistry, Kon-Kuk University, Seoul 143-701, Korea

³Department of Physics, Kent State University, Kent, Ohio 44242, USA

⁴AMLCD, Semiconductor, SEC, KyungGi-do 449-711, Korea

We have studied dielectric properties in the smectic phases of 4-(6-ethoxy-1-trifluoromethyl-hexyloxycarbonyl)-phenyl-4-Nonyloxybiphenyl-4-carboxylat (TFMEOHPNBC) having fluorine attached to one of its benzene rings. Homogeneous and homeotropic 1.5 and 5 μ m thick test cells were prepared to analyze molecular dynamic property. We measured capacitance as a function of temperature in the frequency range between 20 Hz and 100 kHz by using HP4284A LCR meter. We observed that the homogeneous cell has high dielectric constant causing dipole moment in smectic C* phase, but we can see the dipole moments are canceled out in antiferroelectric phase. It is found that there are two kind of the relaxation director fluctuation below 100 kHz. The first is ionic or space charge contribution below 10 Hz, and the second is Goldstone mode near 1~2 kHz. We will discuss molecular dynamics in smectic phase from extra information such as x-ray and electro-optic data.

1. Introduction

Dielectric spectroscopy provides useful information for describing the motion of polar molecules. It is especially important to know not only the ferroelectric torque responsible for the switching between different states, but also the dielectric torque that may cooperate or counteract the ferroelectric torque during different phases of the switching. For the dynamics of director in smectic phase, dielectric data is one of the most important information. In the nematic and SmA phases, the local dielectric properties can be presented by an ellipsoid of uniaxially, with $\epsilon_a \neq \epsilon_b = \epsilon_c$, the principal axis being parallel to the helical axis. The dielectric permittivity tensor has two nonzero components that can be measured in parallel(ϵ_{\parallel}) and perpendicular(ϵ_{\perp}) to the director \mathbf{n} . The dielectric anisotropy $\Delta\epsilon$ is defined as $\epsilon_{\parallel} - \epsilon_{\perp}$. But, the local dielectric ellipsoid is biaxial, $\epsilon_a \neq \epsilon_b \neq \epsilon_c$, with the principal axis making an angle Θ to the helical axis in the SmC* phase. The usual definition of dielectric anisotropy does not fit in the case of tilted smectic phases because of the two non-degenerate

components corresponding to ϵ_{\perp} .

In order to describe the smectic C* phase, there is the dielectric response of the system of two modes of lower frequency connected to the relaxation of director fluctuations. The first one is a fluctuation in the tilt angle (θ) called soft mode and the second is a fluctuation in the azimuthal angle (ϕ) called Goldstone mode. In this dielectric spectroscopy study, at first, we measured and analyzed the temperature dependence of the dielectric constant as a function of electric field and frequency with different cell gap samples. Next, the frequency dependence of the real and imaginary dielectric constant was measured as a function of different cell gap, phases (SmC* and SmC_A) and an electric treatment. Finally, we calculated and analyzed dielectric biaxiality and anisotropy by using the experimental data and simulated director motion in our samples.

2. Experimental

We prepared the 1.5 μ m and 5.0 μ m thick cell of the

anti-parallel rubbed homogeneous samples and also the 4.1 μm thick cell of homeotropic sample. For the homogeneous cells, RN1199 polyimide made by Nissan Chemicals was used, which has 1.1° low pretilt angle. The spin coated polyimide layer on the ITO (Indium Tin Oxide) coated glass substrates were baked at 200 °C for 1 hour, and rubbed manually. The cell was assembled by anti-parallel rubbing direction and fixed the gap by using 5 minute epoxy. Silica spacers were used for 5 μm cell gap control sample and the patterned organic insulator is used as 1.5 μm thick spacer to maintain good cell gap uniformity. After that, the liquid crystal was filled by capillary method at isotropic temperature. Finally, electrodes were connected to ITO coated glass substrates by using indium soldering. For the homeotropic cell, we used the cells which was made by a company for VA(Vertical alignment) test sample. In all of the dielectric measurements, the temperature of the samples was controlled with an absolute accuracy of ± 0.5 °C and a relative accuracy of ± 0.1 °C by use of the oven (model STC200 by Instec Technology Instruments). The values of capacitance for dielectric constant and resistance for dielectric loss (imaginary part of dielectric constant) were measured by using HP4284 LCR meter. The real and imaginary dielectric constant were calculated by using the below.

$$\epsilon' = \frac{C_p \times d}{\epsilon_0 \times A} = \frac{C_p}{C_0}$$

$$\epsilon'' = \frac{d}{2\pi f \times \epsilon_0 \times R_p \times A} = \frac{1}{2\pi f \times R_p \times C_0}$$

where C_p is the measured capacitance of the cell filled with liquid crystal, C_0 is the empty cell capacitance, ϵ_0 is the permittivity of free space (8.854×10^{-12} C/Vm), f is the measuring frequency, R_p is the measured resistance of the cell filled with liquid crystal, d is the cell gap of the sample, and A is the electrode area of the cell. All the measurements of capacitance were performed during cooling scans from isotropic temperature.

3. Results and Discussion

The temperature dependence of the dielectric constants was measured in the frequency region between 20 and 100kHz with 1.5 and 5.0 μm thick homogeneous alignment cells. For 1.5 μm cell, the directors of the liquid crystals in smectic A phase arrange parallel to the substrates. The dielectric constant increases steeply at the

smectic A to C* phase transition temperature, and then it decreases smoothly with stabilize smectic C* phase. At the phase transition point, a sharp peak for the dielectric is observed in the entire frequency region. This can be explained in terms of a soft mode contribution. The high dielectric in the smectic C* phase is caused by Goldstone mode in which the spontaneous polarization contribute the dielectric characteristics due to the helix arrangement. The decrease of the dielectric constant in smectic C* region with decreasing temperature is much larger at lower frequency. It can also be explained that there is charge accumulation or ionic contribution normally occurring below 100 Hz. The dielectric constant in smectic C* phase above 10 kHz is relaxed and reduced because the Goldstone mode is not contributed.

In smectic C_A phase, we can see the dielectric reduced to the value of 7 (almost the same value as in smectic A phase) due to the Goldstone mode. It should not essentially be detectable, since the directors of the liquid crystals are arranged in the kind of herring-bone pattern, i.e. the molecules in neighboring layer tilt to opposite directions and the spontaneous polarization is canceled out. The value of dielectric constant is observed independently below 1 kHz unlike in smectic A and C* phases.

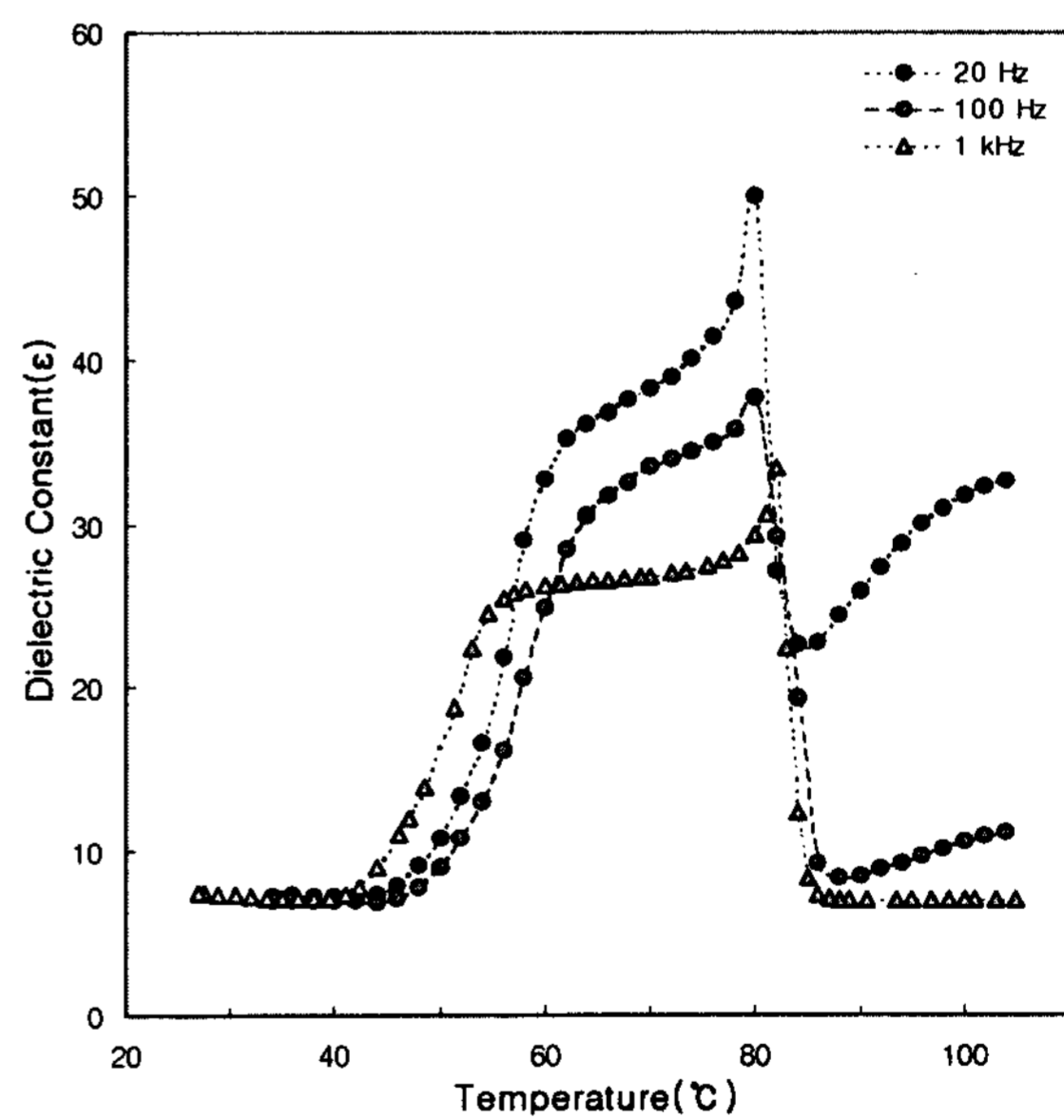


Fig. 1. Temperature dependence of the dielectric constant for 1.5 μm cell gap sample.

The dielectric characteristics at a homogeneous 5 μm thick cell was measured for defining phase transition temperature in other to compare with different boundary contribution in Fig. 2. We can see that there are three critical phases and the smectic C* to smectic C_A phase

transition temperature is different to 1.5 μm thick cell measurement. The high dielectric constant is observed in the region between 72 ~ 86 $^{\circ}\text{C}$ but the smectic C* phase is in 47 ~ 86 $^{\circ}\text{C}$ from other information. The dielectric constant increases with decreasing frequency.

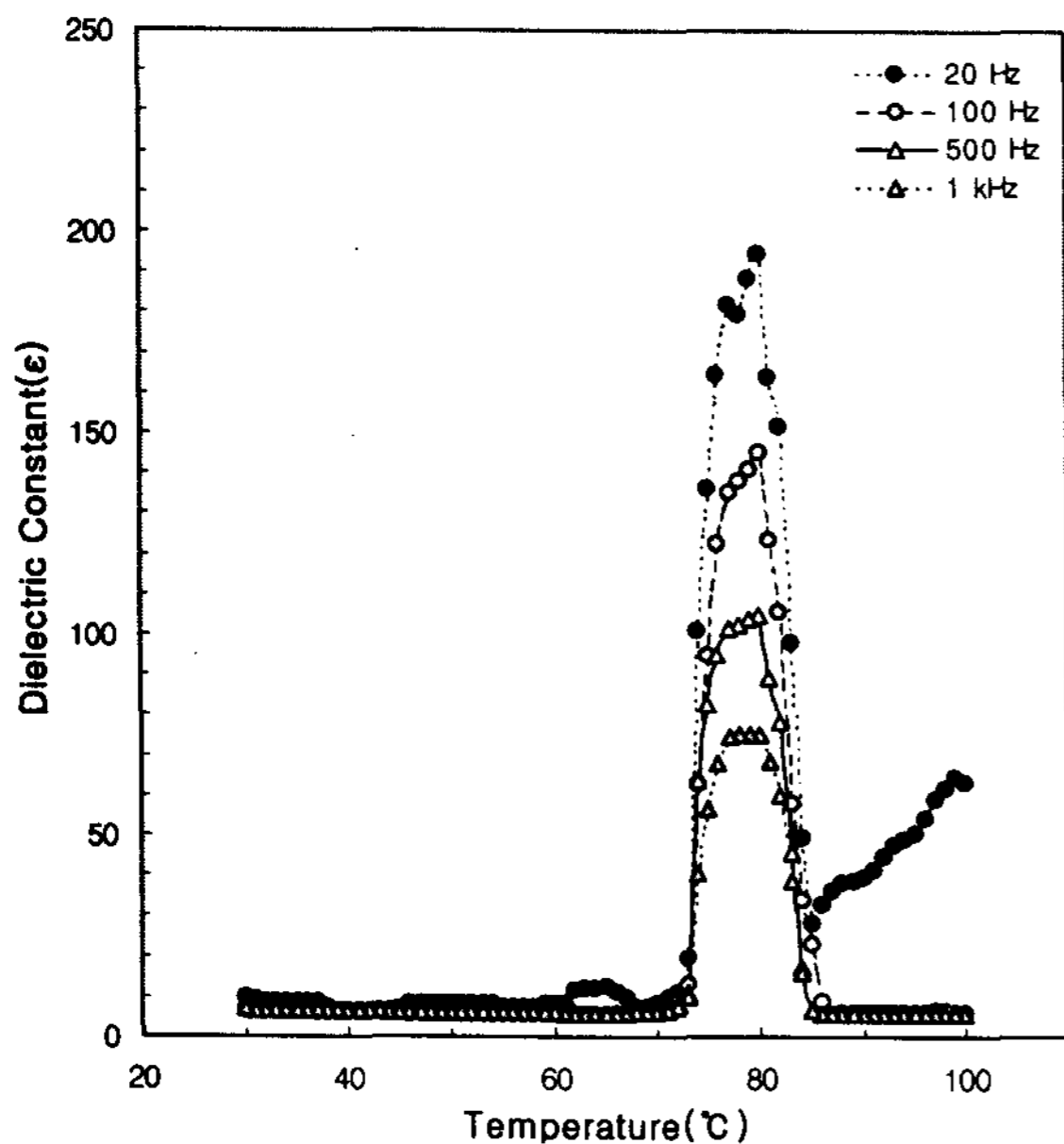


Fig. 2. Temperature dependence of the dielectric constant for 5.0 μm cell gap sample

The real and imaginary dielectric constant were calculated by measuring capacitance and resistance of 1.5 μm and 5.0 μm thick cells. Low (below 100Hz) frequency dielectric relaxation process is detected in SmC* phase, due to the charge accumulation between the polymer layer and the ferroelectric liquid crystal material as shown in Fig. 3. So the charge accumulation phenomenon has been clearly detected by the dielectric relaxation method.

It is well known that with a planar alignment the electric permittivity is due to the collective dielectric processes such as the Goldstone mode, which arises from phase fluctuation, and the soft mode due to the amplitude fluctuation in the tilt angle of the molecules. The Goldstone mode is dominant over the whole SmC* phase for lower frequencies, whereas the soft mode appears at higher frequencies (~100kHz) near the SmC*-SmA phase transition. The electric permittivity is very high below several kHz and decreases with temperature in the SmC* phase, due to the Goldstone mode contribution. The third contribution to the dielectric permittivity is below 100Hz frequency and its intensity is temperature dependent. This means that there is a dielectric relaxation process which is very slow and could either due to the unwinding mode or

a surface effect from the charge accumulated on the surface of the cell, as studied by Biradar *et al.*[4].

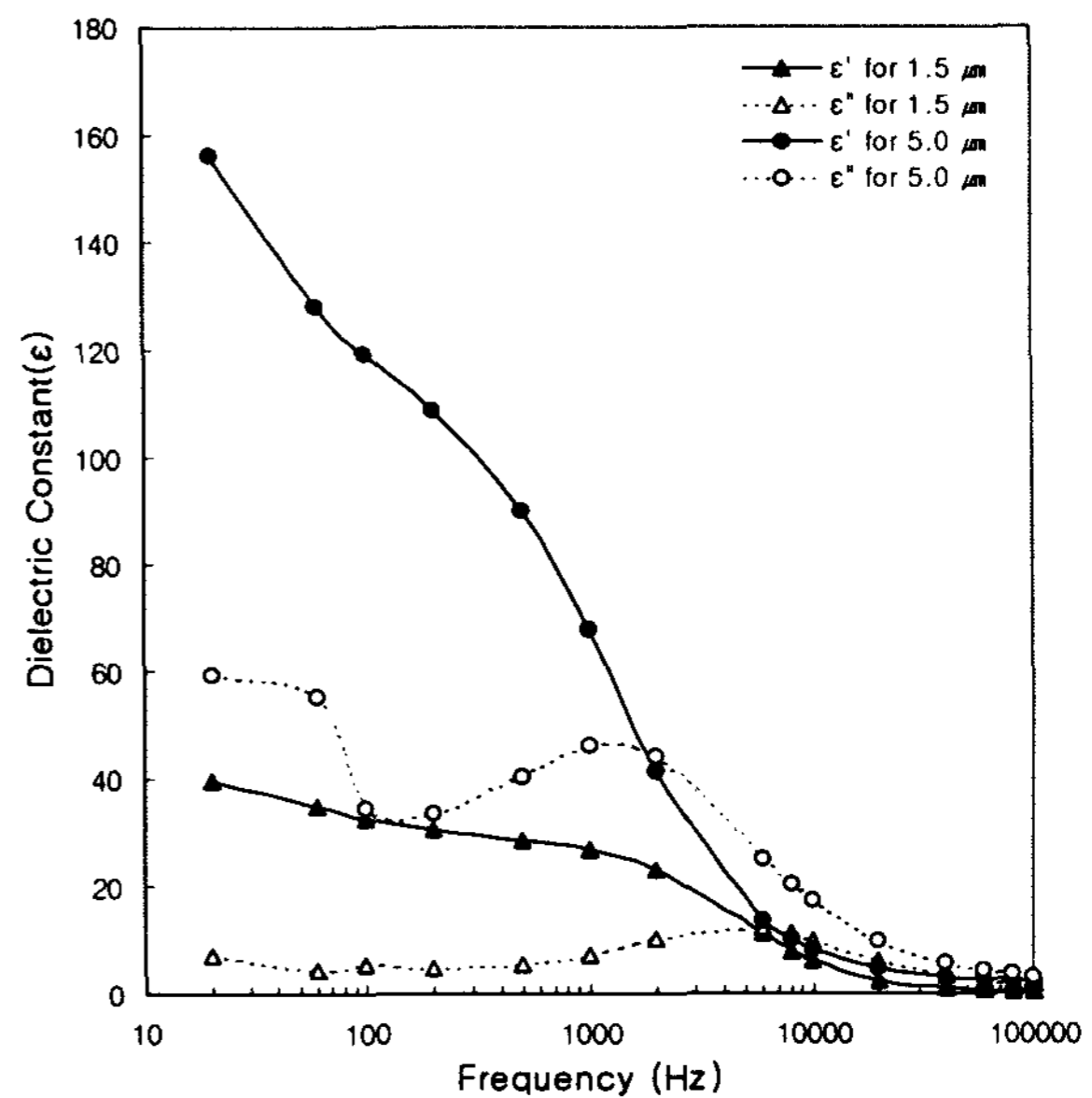


Fig. 3. Frequency dependence of the real and imaginary dielectric constant for 1.5 and 5.0 μm cell gap samples at 75 $^{\circ}\text{C}$ (SmC* phase)

The values of ϵ_1 , ϵ_2 and ϵ_3 were calculated by using the equations in [2][3], the layer tilt angle δ and the director tilt angle Θ have to be determined at different temperatures in the smectic C* and C_A phases. The layer tilt angle δ and the director tilt angle Θ were obtained from x-ray result and polarized microscope respectively. For a homeotropic cell in the smectic A phase, the measuring electric field is then parallel to the director, thus permitting direct measurement of ϵ_{\parallel} . By cooling down to smectic C* and C_A phases, the measuring electric field makes an angle with the director and the measured dielectric permittivity is a mixture of contribution from ϵ_1 and ϵ_3 , which denote ϵ_{hom} .

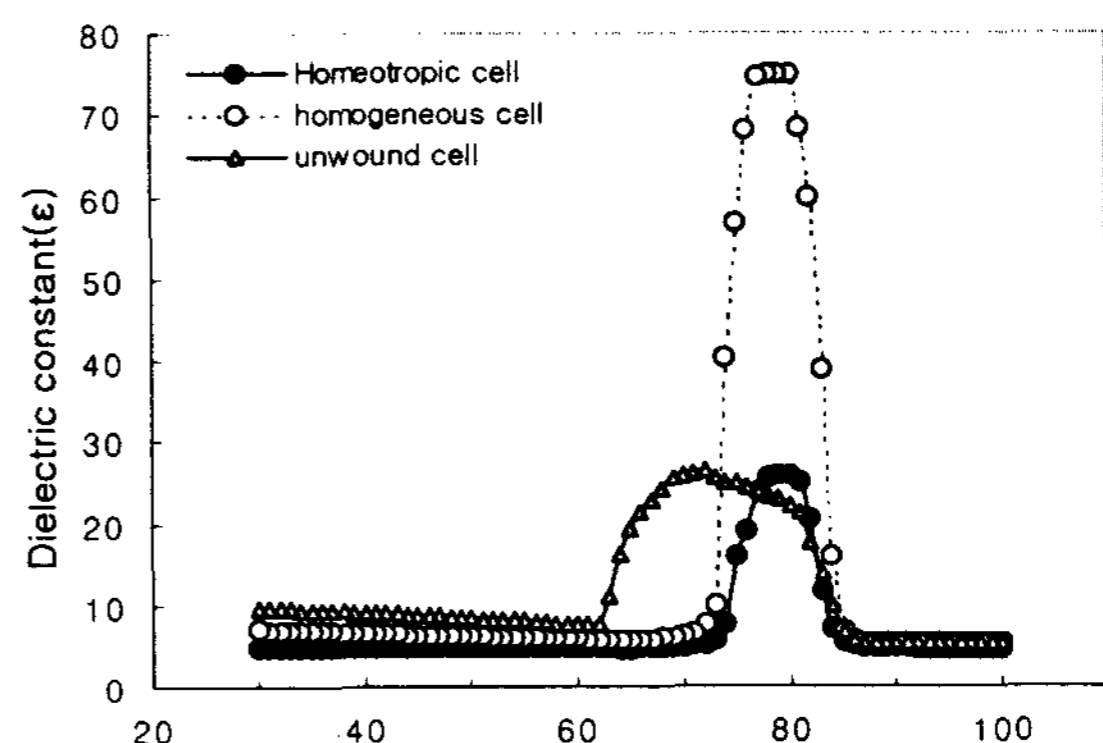


Fig. 4. Temperature dependence of the dielectric constant for homogeneous, homeotropic and unwound cell at 1 kHz.

As shown in Fig. 4, the values of dielectric constant at 1 kHz of low frequency were almost the same as 5.08 and 4.84 at 86 °C (SmA) and 40 °C (SmC_A), respectively. In the homogeneous cell, we can measure the electric field of perpendicular to the director in the smectic A phase, ϵ_{\perp} . In the smectic C* and C_A phases, the measurement result denoted as ϵ_{helix} was the presence of the helix. The temperature dependence of the determined values of ϵ_1 , ϵ_2 and ϵ_3 at low(1 kHz) in Fig 5. As a result, we can get the dielectric anisotropy of below 1 and the dielectric biaxiality of 6.1 with the frequency of 1 kHz at room temperature.

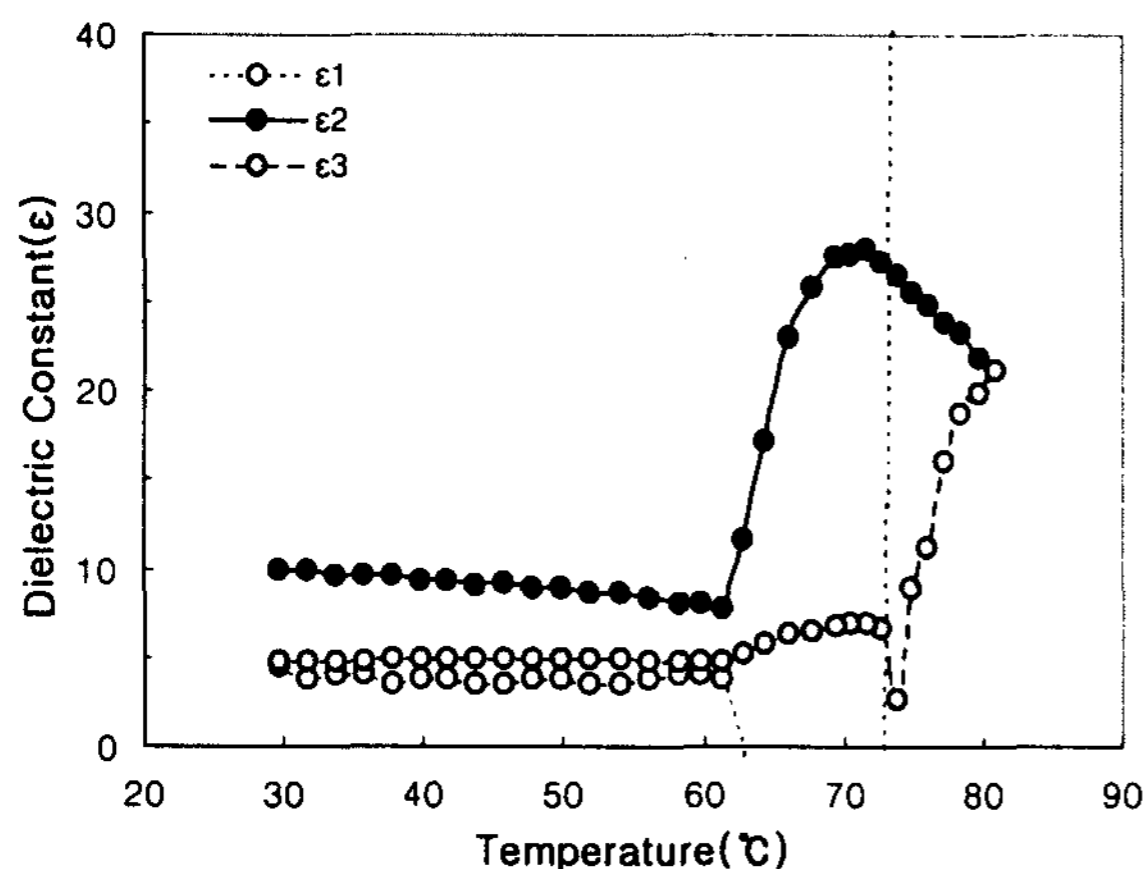


Fig. 5. Temperature dependence of the dielectric constant ϵ_1 , ϵ_2 and ϵ_3 in smectic C* and C_A phases from homogeneous, homeotropic and unwound cell at 1 kHz

This both positive values of dielectric anisotropy and biaxiality at 1 KHz are consistent with previous study [5] i.e $\epsilon_2 > \epsilon_3 > \epsilon_1$. At low frequency of 1 kHz, the dielectric anisotropy was positive and its magnitude much less than the dielectric biaxiality $\delta \epsilon$.

4. Conclusions

The ionic and ferroelectric relaxation frequencies of TFMEOHPNBC were obtained at below 100 Hz and 10 kHz respectively. It is found that the molecular arrangement is depended on the cell thickness in the region of between 48 ~ 72 °C. We can guess the region is antiferro like smectic C phase. High dielectric biaxiality of 6.1 was obtained in room temperature from the homogeneous and homeotropic cells. The high value of dielectric biaxiality is causing the layer reorientation induced electric field. The dielectric anisotropy and biaxiality at 1 KHz have the positive value and the relation is $\epsilon_2 > \epsilon_3 > \epsilon_1$.

Acknowledgement

This work was performed Advanced Backbone IT technology development project supported by Ministry of Information & Communication in republic of Korea.

References

- [1] Z. Xue, M. A. Handschy and N. A. Clark, *Ferroelectrics*, **73**, 305 (1986).
- [2] F. Gouda, G. Anderson, M. Matuszczyk, T. Matuszczyk, K. Skarp and S. T. Lagerwall, *J. Appl. Phys.*, **67**, 180 (1990).
- [3] T. Carlsson, B. Zeks, C. Filipic and A. Levstik, *Phys. Rev. A*, **42**, No.2, 877 (1990).
- [4] A. M. Biradar, D. Kilian, S. Wrobel and W. Haase, *Liquid Crystals*, **27**, No.2, 225 (2000).
- [5] G. Gouda, W. Kuczynski, S. T. Lagerwall, M. Matuszczyk, K. Skarp, *Phys. Rev. A*, **46**, 951 (1992).